2P5-18

Primary experiment for photoacoustic human in vivo tissue strain imaging

光超音波を用いたヒト組織 in vivo 歪イメージングの初期実験

Chikayoshi Sumi[1†] and Naoto Sato[2] ([1]Faculty of Sci. & Tech., Sophia Univ.; [2]R&D dept., CYBERDYNE Inc.)

炭　親良 [1†]，佐藤　直人 [2] ([1] 上智大学理工, [2]CYBERDYNE 研究開発部門)

1. Introduction

Sumi et al have been developing ultrasonic (US) echo human tissue displacement vector measurement methods such as the multidimensional cross-spectrum phase gradient method (CSPGM) [1], the multidimensional autocorrelation method (AM) [2], etc. The methods have also been used for measuring and imaging of strain tensors and shear moduli of *in vivo* breast, liver, heart etc [3]. In ref. 4, the strain measurements were also performed both for photoacoustic (PA) and rf-echo signals obtained from a human *in vivo* wrist (our first trial [5]). A *real-time* PA and rf-echo imaging instrument (AcousticX, CYBERDYNE Inc., Ibaraki, Japan) was used. The layered structures of skin, vein, soft tissue and artery were successfully imaged by both axial strain imagings using the 2-dimensional (2D) CSPGM having a substantial robustness with respect to a signal noise [2]. The PA signals yielded higher axial resolution and higher contrast strain images than rf-echo signals. And, the lateral resolutions and lateral contrasts were also examined for the corresponding PA and echo images. It was confirmed that the PA signal generations depend on tissue types such as a skin and a blood.

In this report, for the strain measurement, the 2D AM with a fewer calculations but with less robustness for a signal noise than the 2D CSPGM [2] is used. And, the spatial resolutions and contrats are more specifically examined for PA and echo images, i.e., including axial ones.

2. Methods

PA signals were acquired from a human *in vivo* left wrist using the AcousticX [4,5]. It was simpler to simultaneously image an artery and a vein than from a finger. The PA system had two 850nm-LED linear array sources which radiated near-infrared light from both elevational sides of an ultrasound 7MHz linear-array probe. The pulse length of light was 35ns and one LED array energy per one pulse was 200μJ. Alternately, US rf-echo data were also acquired by US 10MHz plane wave transmissions.

A research subject was male and 49 years old. The tissue displacement vectors/strain tensors were measured from the PA and rf-echo signals using the 2D AM. The 2D CSPGM allows performing a matched filtering on the signals during a displacement measurement and then, the method yields a considerably high accuracy measurement with a substantial robustness with respect to a noise signal. Alternatively, the 2D AM allows a real-time measurement, and the similar high accuracy only when the signals have a high signal-to-noise ratio (SNR). Analogue rf-echo and PA signals were amplified with gains of 52 and 106 dB, respectively. Because the SNRs of PA signals were much lower than those of rf-echo signals, addition averaging was performed for PA signals (N = 256). For superposed, PA and B-mode imaging, an achieved frame rate was 16Hz.

3. Experiments

Fig. 1a shows a superposed, PA and B-mode image [4]. Moreover, **Fig. 1b** shows a gray-scaled image of an axial strain obtained from a pair of successive rf-echo data frames and **Fig. 1c** shows two axial strain images obtained from two pairs of successive PA data frames, which were obtained using the 2D CSPGM [4]. The strain images are snapshots with different times. However, the tissue structures were visualized similarly with high correlations between the images, i.e., the skin, vein with vessels, soft tissue, artery with vessels. As shown, the strain images obtained from PA data had a higher axial resolution and a higher contrast than that obtained from rf-echo data [4].

Next, **Fig. 2a** and **2b** respectively show strain images newly obtained from the same rf-echo and PA data using the 2D AM. Increasing of the SNRs of PA data owing to the addition averaging and decreasing of a local window for the displacement measurement increased the measurement accuracy and a spatial resolution, although the stability was still lower than that of 2D CSPGM results.

Fig. 3 shows for the PA and rf-echo data at the positions of a skin and, a vein and an artery,

the 2D point spread functions (PSFs) of non-beamformed, received, raw data, which were estimated using normalized 2D autocorrelation functions. Usually, an addition-averaged PSF is shown at each depth, the data are not averaged ones. The rf-echo data yielded almost same PSFs regardless the depth, particularly for the venous and arterial blood. In contrast, the PA data yielded characteristic PSFs and spectra (omitted), being dependent on the tissue types including neighboring tissue types, and tissue compositions, structures, geometries and sizes. The PA signal generation in the skin (epidermis), and vein and artery are respectively caused by the existence of a melanin and a blood. The PA data generated in the tissues had lower center frequencies than the corresponding rf-echo data. The PA data generated in the skin had a smaller axial bandwidth than those generated in other tissues, specifically, not having very low frequency spectra including a DC and not having higher frequency spectra. Interestingly, an arterial blood had a larger axial bandwidth than the venous blood. The PA data generated in the skin and blood in the neighborhoods of vessels had small lateral bandwidth. It was also confirmed that artifacts of multiple PA reflections/scatterings significantly occurred at weak PA generation regions such as a water and a hypodermis (Fig. 1) and a blood (Fig. 3).

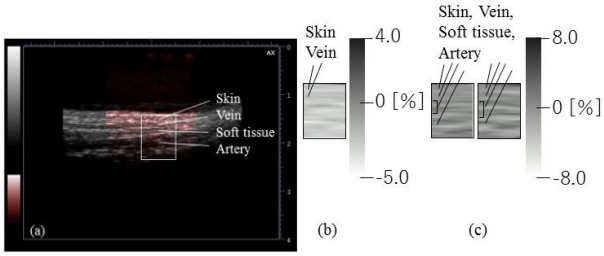

Fig. 1. (a) Superposition of PA and B-mode images; and gray-scaled axial strain images obatined using 2D CSPGM from (b) rf-echo and (c) PA data with different times [4].

4. Conclusions

Similarly to the 2D cross-spectrum phase gradient method [4,5], the 2D autocorrelation method (2D AM) successfully yielded the axial strain images from the human *in vivo* wrist PA data. The layered structure of a skin, a vein, a soft tissue and an artery were successfully visualized. Also with 2D AM, the strain imaging had a higher axial resolution and a higher axial contrast than those performed for rf-echo data. At the symposium, the lateral strain image data will also be presented. Although the lateral displacement/velocity was able to be measured, the lateral strain measurements became slightly unstable. In the near future, various

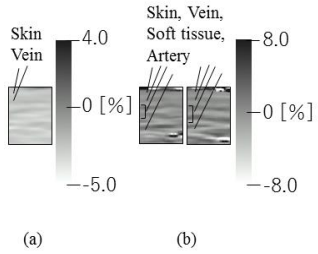

Fig. 2. Gray-scaled axial strain images obtained using 2D AM from the same (a) rf-echo and (b) PA data as those of Fig. 1.

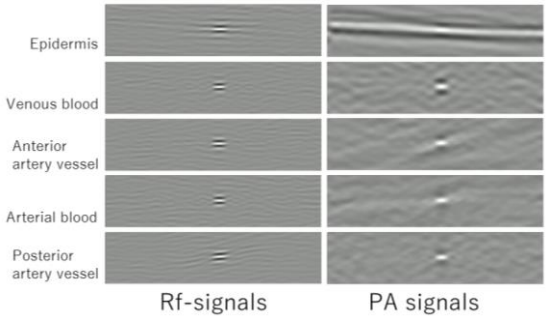

Fig. 3. Normalized 2D PSFs obtained for PA and rf-echo data at skin, vein and artery (anterior vessel, arterial blood and posterior vessel).

lateral modulation reception beamformings will be performed. The differences between PA and rf-echo signals caused by tissue types (skin and blood) were also specifically examined by estimating a PSF and spectra. The above-mentioned tissue types etc. have influences on a resolution and a contrast of a PA image significantly. Such estimations will also be useful for differentiating malignant tissues.

At the symposium, the results of PA signals generated for representative PA materials such as a bovine blood, an emulsion and an indocyanine green (ICG) etc. will be presented additionally. Dependencies of PA generations on a temperature will also be addressed toward the monitoring applications to HIFU treatments for superficial tissues and organs directly. In the near future, the same frequency LEDs will be added to increase PA SNRs at desirable positions; and different frequency LEDs (e.g., 690nm) will also be used to perform estimations of frequency variances. A focused light will also be used to increase a lateral resolution and a lateral contrast.

References

1. C. Sumi: IEEE Trans. UFFC **46** (1999) 158.
2. C. Sumi: IEEE Trans UFFC **55** (2008) 24.
3. C. Sumi: IEEE Trans UFFC **52** (2005) 1670.
4. C. Sumi and N. Sato: "Photoacoustic strain imaging on human *in vivo* wrist" in Proc 38th IEEE EMBC (2018).
5. C. Sumi and N. Sato: JJMU **45(suppl)** (2018) S579 [in Japanese].